ELSEVIER

Applied Acoustics 64 (2003) 1–23

applied acoustics

www.elsevier.com/locate/apacoust

An improved model to predict energy-based acoustic parameters in Apulian-Romanesque churches

E. Cirillo, F. Martellotta*

Dipartimento di Fisica Tecnica, Politecnico di Bari, via Orabona 4, I-70125 Bari, Italy

Received 4 March 2002; received in revised form 23 July 2002; accepted 24 July 2002

Abstract

In this paper an improved model to predict energy relations in churches is proposed. A detailed acoustic survey was carried out of nine Romanesque churches having volumes ranging from 33 000 to 1500 m^3. The measured sound level and early/late ratio showed significant correlation with the source–receiver distance, but the comparison with values predicted using theoretical models initially gave unsatisfactory results. The main difference was due to the early energy which was underestimated at points near the source and overestimated at distant points. Barron's revised theory proved to be the most reliable among the analysed models, so, in order to improve its prediction accuracy, a modified early reflected energy component was added to the direct and reverberant sound. The improved model was finally validated and the comparison between predicted and measured values gave good results.

Keywords: Acoustic parameters; Prediction; Revised theory; Churches

PACS: 43.55.Gx; 43.55.Br

1. Introduction

Churches and other places of worship are gaining more and more importance from the acoustic point of view. Several papers have been published, most of which deal with reverberation time [1–4], but more recent works have also investigated

* Corresponding author. Tel.: +39-080-596-3631; fax: +39-080-596-3419.
E-mail address: f.martellotta@iol.it (F. Martellotta).

0003-682X/02/$ - see front matter
PII: S0003-682X(02)00068-3

other acoustic parameters. In particular, attention has been paid to speech intelligibility [5–7] as well as to sound pressure level and other energy-based indices [8–11], for which models and formulas have even been proposed to predict their values [7,8].

However, the prediction of acoustical parameters in churches is often difficult. In fact, the reverberation time may be calculated, in general, by means of Sabine's formula, but sometimes this relation cannot be applied inside churches because of acoustic coupling effects between different volumes of these complex buildings. Chapels, domes, aisles, and women's galleries may only be partly coupled with the main volume and therefore Sabine's formula is not suitable to predict reverberation time and the energy balance equation needs to be solved [12]. Fortunately, when the geometry is not too complex, acoustic coupling effects are mostly negligible, so the reverberation time may be easily calculated provided that the volume and total surface area have been correctly determined and that absorption coefficients are known with reasonable accuracy.

The prediction of the other acoustic parameters is even more complex because they are more position-sensitive than the reverberation time. Regression analyses show that there are correlations between some acoustic parameters [7,13], but even though the correlations are statistically significant, it is not really useful to calculate the value of a parameter as a function of another one which needs, however, to be measured. Correlations between acoustic parameters and geometrical characteristics, such as the source–receiver distance, are more useful for prediction purposes because acoustic parameters can be calculated knowing only the geometry of the room. However, a set of empirical equations, found in [13] by means of regression analyses, showed that individual location values of energy-based parameters can be predicted, with tolerable approximation, only using both geometrical and acoustic characteristics of a room.

A theoretical model which takes into account both these features of a room was proposed by Barron and Lee [14]. This model, described in more detail in the next section, is widely used to predict strength and clarity in auditoria, but some references [8–11] show that it does not perform well in churches and other places of worship.

An acoustic survey, carried out in some Romanesque catholic churches built in Apulia (Italy) [15] led to similar conclusions, so the collected data were used to propose some corrections to Barron's theory in order to achieve better performance in predicting energy-based acoustic parameters inside this kind of churches. This paper discusses the proposed model, demonstrating that it allows reliable predictions of both the strength factor and clarity index.

2. Theoretical models overview

According to the classical theory of the sound propagation in enclosed rooms [16], if the absorption is uniformly distributed and if the sound field is diffuse, the sound pressure level (in dB) at a point at a distance r from the source (assumed to be omnidirectional) is:

$$L = 10\log\left[\frac{\rho c W}{p_{\mathrm{ref}}^2}\left(\frac{1}{4\pi r^2}+\frac{4}{A}\right)\right]. \tag{1}$$

Where ρ is the air density, c is the speed of sound in air, W is the sound power of the omni-directional source, p_{ref} is the standard reference pressure, and A is the total acoustic absorption of the room. A can be expressed as a function of the reverberation time (RT) and of the room volume (V) by means of Sabine's equation ($A = 0.161V/RT$). If the sound pressure level is measured in terms of the strength index G, that is assuming the level L_0 of the direct sound at a distance of 10 m from the source as a reference, Eq. (1) becomes:

$$L - L_0 = 10\log\left(100/r^2 + 31200V/RT\right). \tag{2}$$

If, according to the classical theory, a perfectly exponential decay is assumed to follow an impulsive excitation, then the instantaneous energy density (in J/m^3) of the reverberant field may be expressed using the following equation ([16], p. 200):

$$g(t) = (W\Delta t/V)\mathrm{e}^{-13.8t/RT}, \tag{3}$$

where Δt is the impulse duration. If $g(t)$ is normalized assuming as a reference the "integrated" energy density of the direct sound at 10 m distance (in Js/m^3):

$$E_{\mathrm{d10}} = (W\Delta t)/(400\pi c), \tag{4}$$

then Eq. (3) becomes:

$$g'(t) = g(t)/E_{\mathrm{d10}} = 13.8\cdot 31200/V\mathrm{e}^{-13.8t/RT}, \tag{5}$$

where $g'(t)$ is expressed in s^{-1}, and becomes dimensionless after integration. In this way all the energy-based acoustic parameters may be calculated according to the diffuse-field theory as a function of RT, V, and r. However, the main drawback of the classical theory is that beyond the reverberation radius the predicted reduction in total level and in every other acoustic parameter is small compared to the measured values.

Barron and Lee [14] proposed a model to account for this behaviour. They noticed that the concert hall situation differed from diffuse requirements in several aspects. However, they found that the sound level decay was linear soon after the direct sound in the majority of the halls, the main discrepancy being observed in the decrease in the reflected sound level with increasing source-receiver distance. So, they proposed a model based on the following assumptions. The direct sound is followed by linear level decay at a rate corresponding to the reverberation time. The instantaneous level of the late decaying sound is uniform throughout the space, so that decay traces are superimposed. The time $t = 0$ corresponds to the time the signal is emitted from the source, therefore the direct sound reaches a point at a distance r

from the source after a time $t_D = r/c$, where c is the sound velocity in air. In this way the integrated energy decreases when the source-receiver distance increases and the early/late energy ratio also behaves similarly. The absolute value for the reflected sound level is assumed to be, at $t = 0$, equal to the value predicted by the classical theory [Eq. (2)].

Under these conditions Barron's integrated energy from time t to infinity corresponds to the dimensionless integral of Eq. (5) over the same time-interval:

$$i_t = (31200RT/V)e^{-13.8/RT}. \tag{6}$$

To predict the total sound-pressure level and early/late ratio the sound energy is divided into three components: the direct sound (d), the early reflected sound (from 0 to 80 ms, e), and the late sound (from 80 ms to infinity, l). From Eq. (6), the corresponding dimensionless energies of each of them become:

$$d = 100/r^2, \tag{7}$$

$$e = (31200RT/V)e^{-0.04r/RT}\left(1 - e^{-1.11/RT}\right), \tag{8}$$

$$l = (31200RT/V)e^{-0.04r/RT}e^{-1.11/RT}. \tag{9}$$

So the strength index (in dB) is given by:

$$G = L - L_0 = 10\log(d + e + l), \tag{10}$$

and the clarity index (in dB) is given by:

$$C_{80} = 10\log[(d + e)/l]. \tag{11}$$

Barron and Lee compared measured and predicted values, proving the suitability of the "revised" theory in many concert halls. They remarked, however, that in the presence of highly diffusing ceilings the model overestimates the results because a steeper early energy decrease is observed.

Sendra et al. [8] observed similar results in Mudejar-Gothic churches and, in order to obtain better predictions, suggested modifying Barron's theory by means of a factor β affecting the arrival time in Eqs. (8) and (9). The factor β was empirically determined by means of non-linear regression analyses in order to maximize the correlation between measured and predicted values of the sound pressure level. This procedure has two drawbacks. The first is that different values of β are defined for each church and for each frequency band taken into account, even if compromise average values are proposed as well. The second is that the early/late energy ratio prediction proves to be unreliable [9,11].

A more general model, based on Barron's theory, but applied to halls with asymmetrical absorption, was proposed by Arau [17]. In this model the sound decay is divided into three parts with different slopes, corresponding to the early, early reverberant and late reverberant sound. The latter is generally negligible because of

its low energy, while the first two are influenced respectively by the initial decay time (T_i) and by the mean reverberation time (T). If T_i and T are equal, the model provides the same results as Barron's. However, in addition to a certain mathematical complexity, this model depends on the knowledge of some position-sensitive parameters which, like the initial reverberation time, need to be measured.

Other formulas, such as those proposed by Gade [18], take into account only average room values and are based on regression analysis.

To conclude this overview, it appears that the only model able to provide a general and theoretical approach is Barron's one, therefore the model proposed in this paper is based on it.

3. The acoustic survey

3.1. The churches surveyed

Nine Catholic churches built in Apulia (Italy) in Romanesque style were analysed in detail during an acoustic survey [15]. The churches have different geometrical characteristics, summarized in Table 1. From the architectural point of view the churches share some common features, such as the plan of the basilica, with a main nave and side aisles, a marble floor with wooden pews, and hard limestone walls and columns. Nonetheless, they have specific features, briefly described below.

St. Nicholas Basilica in Bari (Figs. 1a, 2a, 3) is the prototype of the Apulian Romanesque style, it has a transept with three apses. Two columns separate the transept and the nave. There are roofed women's galleries, while the nave ceiling is wooden with large painted canvases. The side aisles are cross-vaulted.

Bari Cathedral (Figs. 1b, 4a) has a transept with three apses and a dome over the crossing. The remaining part of the church has a wooden roof with trusses. There are false women's galleries, therefore the side aisles are roofed and higher than in St. Nicholas.

Bitonto Cathedral (Fig. 1c) has a transept with three apses. The aisles are cross-vaulted, while the remaining parts are roofed with trusses.

Table 1
Basic details of the nine churches surveyed

Church	Volume (m^3)	Floor area (m^2)	Total area (m^2)	Length (m)	RT_{mid} (s)
St. Nicholas Basilica, Bari	32 000	1530	10 500	54	4.4
Bari Cathedral	30 100	1274	9500	46	5.3
Bitonto Cathedral	16 000	858	6500	42	4.3
Barletta Cathedral	15 800	912	5500	46	6.8
Bisceglie Cathedral	10 150	534	4660	29	3.5
Ruvo Cathedral	6400	445	3000	29	3.7
Bovino Cathedral	3840	452	2420	22	3.8
Ognissanti church, Valenzano	1800	258	1300	19	5.4
Vallisa church, Bari	1520	162	1130	15	2.1

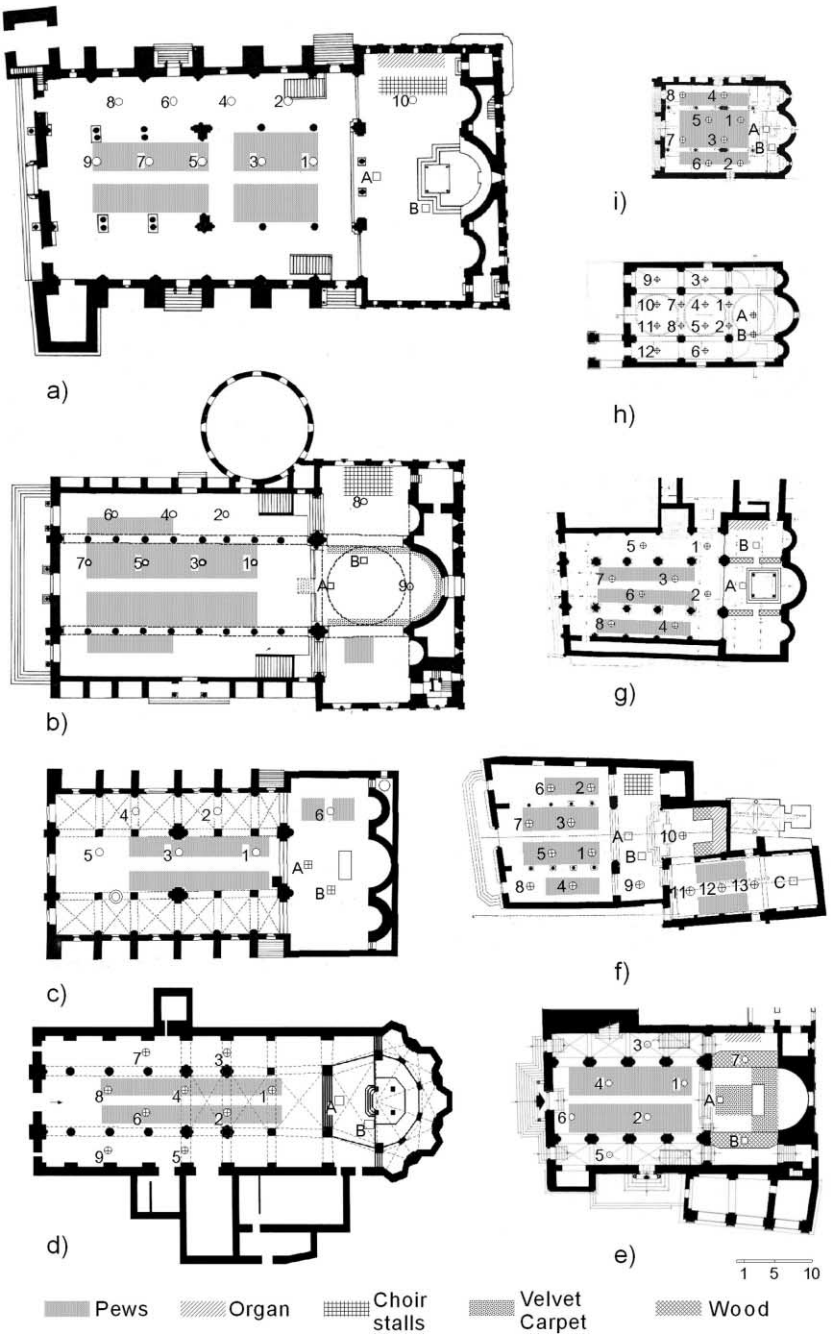

Fig. 1. Plans of the churches surveyed: (a) St. Nicholas Basilica; (b) Bari Cathedral; (c) Bitonto Cathedral; (d) Barletta Cathedral; (e) Bisceglie Cathedral; (f) Bovino cathedral; (g) Ruvo Cathedral; (h) Ognissanti Church; (i) Vallisa Church. (○) receiver positions, (□) source positions.

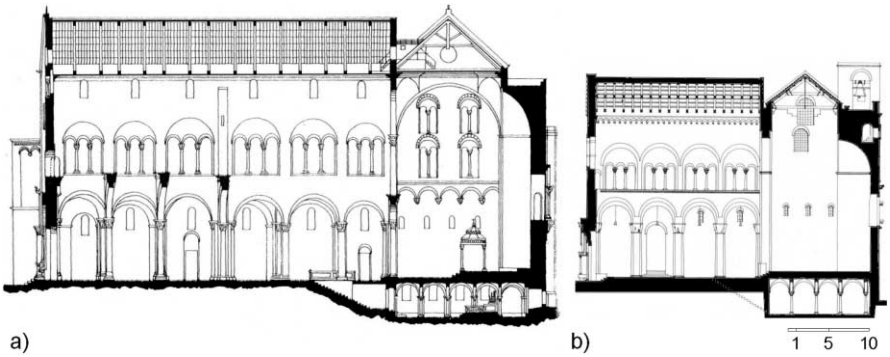

Fig. 2. Long sections of (a) St. Nicholas Basilica, and (b) Bisceglie Cathedral.

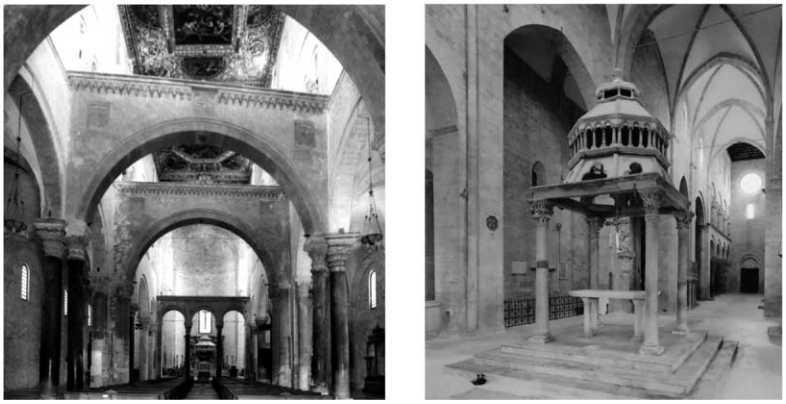

Fig. 3. Pictures of (a) St. Nicholas Basilica, and (b) Barletta Cathedral.

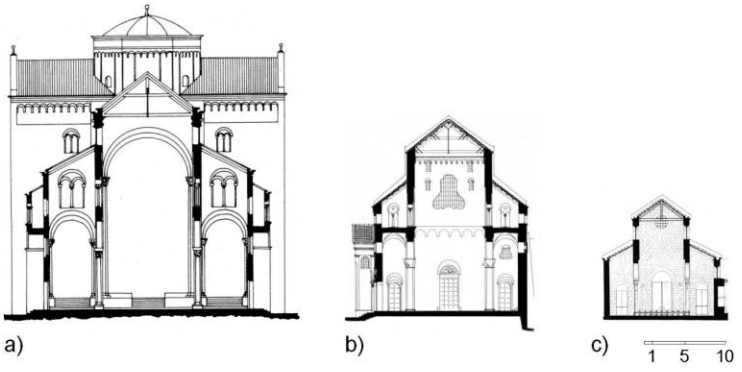

Fig. 4. Cross sections of (a) Bari Cathedral, (b) Bisceglie Cathedral, and (c) Vallisa Church.

Barletta Cathedral (Figs. 1d, 3) is made of two parts, on the facade side it is Romanesque with wooden roofs, and on the chancel side it is Gothic with ribbed cross-vaults on large pillars. There is no transept but there is a Gothic choir with radial chapels.

Bisceglie Cathedral (Figs. 1e, 2b, 4b) has a transept with a large central apse and wooden stalls on both the sides and carpets on the chancel floor. Since there are false women's galleries the aisles are roofed as is the nave.

Ruvo Cathedral (Fig. 1f) has a transept with three apses. There are no women's galleries and the aisles are cross-vaulted. The nave and the transept are roofed with trusses.

Bovino Cathedral (Fig. 1g) has a transept with a vaulted choir. There are no women's galleries and both the nave, and the aisles are roofed. The walls are plastered.

Ognissanti church (Fig. 1h) has no transept but it has apses. The nave is vaulted with three domes, while the aisles are barrel-vaulted. Because of restoration work the floor is currently made of concrete and there are no pews.

Vallisa church (Figs. 1i, 4c) has three apses, without a transept. Both the nave and the aisles are roofed with trusses. Since the church is used as an auditorium there are lightly upholstered seats instead of pews. The chancel area is used as a stage and is made of wood on wooden joists.

3.2. Measurement technique

The measurements were carried out using an omni-directional sound source made of twelve 100 mm loudspeakers mounted on a dodecahedron driven by a 300 W amplifier. A GRAS 40-AR omni-directional microphone was used together with a 01 dB Symphonie system installed on a laptop computer. An MLS signal was used to excite the rooms. The order of the signal was adapted to the reverberation characteristics of each room to avoid time-aliasing problems and each MLS sequence was repeated 32 times to improve the signal-to-noise ratio.

In each church at least two source positions were used, one on the axis of symmetry and one off the axis, both in the chancel area. The source was placed 1.5 m above the floor. Nine receiver positions were used on average. In very large but symmetrical churches the receivers were only placed in one half of the floor, otherwise they were spread to cover the whole floor area uniformly. The microphone was placed 1.2 m from the floor surface.

All the measurements and the calculations of the indices were carried out according to ISO-3382 standard [19]. In particular for the measurement of the strength index (G) the sound power of the source was calibrated in a reverberation chamber, employing the same measurement chain and the same settings used during the on site survey.

4. Experimental results

The analysis of the results showed that, in each church, the energy-based indices and source–receiver distance were significantly correlated (see Fig. 5). The existence of such correlations supported the idea that more general equations could be found

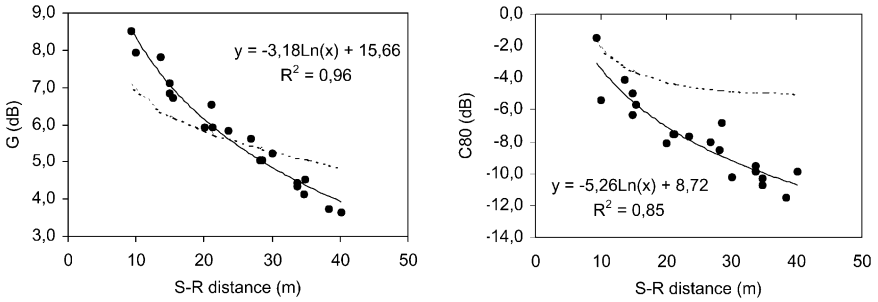

Fig. 5. Plot of measured (•) and predicted values by Barron's (- - -) of the strength index (left) and early/late ratio (right) at 1 kHz inside St. Nicholas Basilica vs source-receiver distance. (—) regression lines.

to predict energy-based indices as a function of a simple geometrical parameter as the source–receiver distance.

Predicted and measured values of the strength index and early/late ratio were compared to estimate the reliability of Barron's theory inside churches. As can be seen in Fig. 5, and in Table 2, the following results were observed:

- the mean values of the strength index were predicted with reasonable accuracy, however the theory tended to underestimate the values at points near the source and to overestimate the values at points far from the source;
- the predicted slope of the strength index was always lower than the measured one. The mean difference was −1.1 dB/10 m, with a minimum of −0.3 dB/10 m and a maximum of −1.9 dB/10 m;

Table 2
Differences between measured and Barron's values of energy-based indices based on linear regression with source–receiver distance

Church	G		C_{80}		Early		Late	
	Mean	Slope	Mean	Slope	Mean	Slope	Mean	Slope
St. Nicholas Basilica, Bari	0.1	−0.8	−3.5	−1.5	−2.9	−2.2	0.6	−0.6
Bari Cathedral	−0.4	−0.7	−2.8	−1.3	−3.0	−1.7	−0.1	−0.6
Bitonto Cathedral	−0.1	−1.2	−1.0	−1.3	−1.1	−2.3	−0.1	−1.0
Barletta Cathedral	−0.4	−1.5	−5.0	−2.3	−4.9	−4.5	0.0	−1.5
Bisceglie Cathedral	0.5	−1.9	−2.0	−2.9	−1.8	−4.6	0.8	−0.2
Ruvo Cathedral	−0.9	−1.6	−1.7	−3.6	−2.6	−4.5	−0.7	−0.6
Bovino Cathedral	−0.4	−1.1	−1.4	−3.0	−2.2	−2.6	−0.4	−0.1
Ognissanti church, Valenzano	−0.3	−0.9	−1.6	−3.7	−2.0	−4.7	−0.1	−0.3
Vallisa church, Bari	−0.6	−0.3	−1.6	−2.5	−1.4	−1.7	0.0	1.0
Mean	−0.3	−1.1	−2.3	−2.5	−2.4	−3.2	0.0	−0.4
Standard deviation	0.4	0.5	1.3	1.0	1.1	1.3	0.5	0.7

Mean level differences (dB) and slope differences (dB/10 m) between measured and theoretical values at 1 kHz frequency band.

- the mean values of the clarity index were systematically overestimated. A similar behaviour was observed in each receiver position, where measured values were often below Barron's curve;
- the predicted slope of the early/late ratio was always lower than the measured one. The mean difference was high, being −2.5 dB/10 m.

The explanation of this behaviour was found through the observation of the plot of the early and late sound level as a function of the source–receiver distance. Fig. 6 and Table 2 show that there was good agreement between predicted and measured late sound levels. On the contrary, the values of the early sound level were considerably overestimated by the theory. According to Barron and Lee [14] a high drop-off of the early level can be due to a highly diffusing ceiling which, in reflecting according to Lambert's Law, sends less energy to the rear of the room (far from the source) than to the front. In the surveyed churches there are trusses on the roof, columns along the nave, arches, niches and other architectural elements (see Figs. 1–4) which scatter the incident sound and, together with the highly reflective source area, might lead to the observed behaviour.

The behaviour of the early sound was further investigated by plotting the early level decay traces of points at different distance from the source. Fig. 7 shows two examples of such curves. First of all it was observed that the reverberant sound field was sufficiently uniform at different points of the room, in fact, the linear parts of each decay curve were nearly coinciding. It appeared, however, that the time at which the decay began to be linear was later, the farther the measurement position was from the source. Then, the early sound and the "ideal" reverberant field, extrapolated by extending the linear part common to all the decay traces, were compared. At points near the source the early reflections brought more energy than the ideal reverberant field, in fact the decay curves were above the extrapolated line. On the contrary, as the distance from the source grew the early reflections became weaker and the decay curves moved below the ideal line. This behaviour influenced the early decay time that in most cases showed a tendency to grow with the source–receiver distance (Fig. 8).

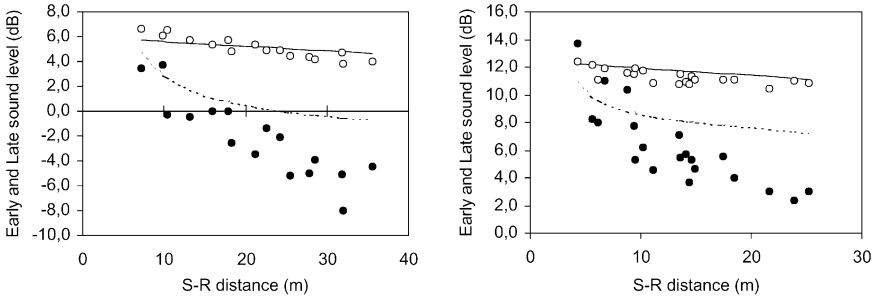

Fig. 6. Plot of predicted (using Barron's model) and measured early and late sound level at 1 kHz octave as a function of the source–receiver distance in Bari Cathedral (left) and Bovino Cathedral (right). (•) measured early level, (- - -) predicted early sound level, (○) measured late sound level, (—) predicted late sound level.

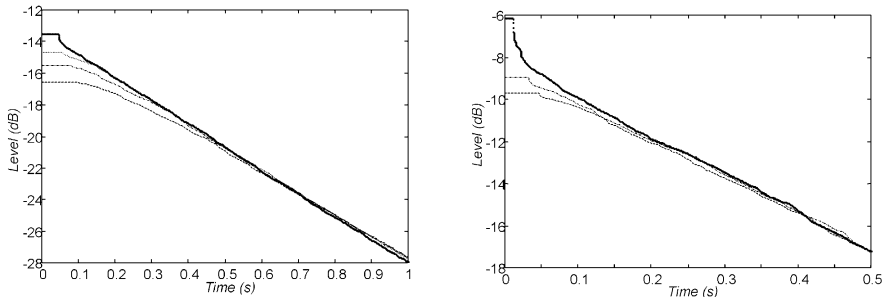

Fig. 7. Integrated impulse response decays at 1 kHz octave, measured in different points of the nave of St. Nicholas Basilica (left) and of Ruvo Cathedral (right). Lower curves correspond to points at increasing

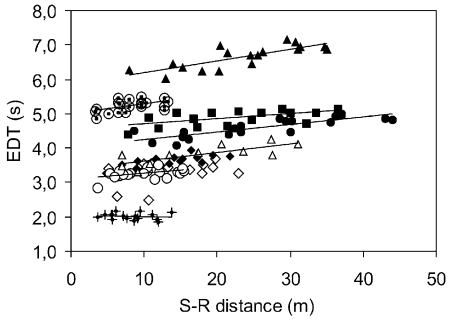

Fig. 8. Plot of the early decay time vs source receiver distance for the 1 kHz octave, in the nine churches. Different symbols correspond to different churches.

5. The improved model

The measurement results, discussed in the previous section, were used to develop a model capable of providing better predictions inside Romanesque churches. The most important consequence was the introduction of an early reflected energy component which fitted the observed results. Two steps were needed to define it.

The first step was to assume the reverberant sound field to be uniform, as it is in Barron's theory. However, to comply with the experimental results, the linear level decay had to start with a certain delay (t_R) after the arrival of the direct sound. The measurements showed that this delay was proportional to the source–receiver distance (Fig. 7), therefore, in general, it could be written as $t_R = \rho r$. A reasonable estimate for ρ was obtained by assuming that the delay at the farthest point could not exceed the time (t_{Rmax}) necessary to have a sufficiently high reflection density (N). This value was estimated by applying the image source method formula which gives the number of mirror sources contained in a shell volume ([20], p. 92), and expressing the time (in seconds) as a function of the room volume, the temporal density of the reflections arriving at that time (assumed equal to 1000 reflections/s), and the sound velocity:

$$t_{\mathrm{Rmax}} = \sqrt{VN/4\pi c^3}. \tag{12}$$

The maximum source–receiver distance $r_{\max}$ was assumed to be equal to the distance between the source and the farthest wall, so ρ was finally given (in s/m) by:

$$\rho = t_{\mathrm{Rmax}}/r_{\max}. \tag{13}$$

Comparisons with measured values showed that, in the presence of many concave surfaces near the source, the sound propagation is hindered and ρ should be increased. On the contrary, when there are few obstacles to sound propagation, as in auditoria, ρ should be decreased. In fact, when ρ tends to zero the proposed model approximates Barron's one.

The second step was to schematise the early reflected sound arriving between the direct sound and the reverberant sound field. This part of the sound decay is characterised by discrete reflections which are spaced in time according to the geometry of the room. The magnitude of these reflections is proportional to that of the direct sound according to the characteristics of the room surfaces.

In order to simplify the model, the energy density of the discrete reflections was quantified by means of a continuous linear function varying from an initial value (at the arrival time of the direct sound t_{D}), given by the energy of the direct sound multiplied by a factor γ, and a final value (at time $t_{\mathrm{D}} + t_{\mathrm{R}}$), equal to the energy density of the reverberant field at the same time. The factor γ was introduced to account for the magnitude of the early reflections compared with the direct sound, and to transform (by means of the early reflection density ϵ) a discrete process into a continuous one.

When sound hits a wall, part of its energy is absorbed and part is scattered, the first is lost, while the second is "distributed" in time and space. Therefore, the early reflections are expected to contain only a fraction of the direct sound energy corresponding to the specularly reflected energy. So, the factor γ was assumed to be proportional to $(1-\alpha)(1-\delta)$, where α and δ are, respectively, the mean absorption coefficient and the mean scattering coefficient of the room surfaces. The estimation of the mean scattering coefficient can be somewhat difficult owing to the relative lack of data in the literature. However a rough, but realistic, estimation may be tolerated because the model proved to be fairly immune to small variations of the parameter.

Finally, in order to quantify the energy of the discrete early reflections by means of a continuous linear function, the factor γ had to account for the early reflection density $\epsilon = 1/\Delta\tau$, where $\Delta\tau$ is the average time interval (in seconds) between two consecutive early reflections. A reasonable estimation of the early reflection density ϵ is given by the mean reflection frequency, calculated according to the classical diffuse-field theory as the ratio between the sound velocity in air c, and the mean free path (MFP) equal to $4V/S$, where V is the room volume and S is the room surface area. In conclusion, the factor γ is given (in s^{-1}) by:

$$\gamma = \epsilon(1-\alpha)(1-\delta) = (cS/4V)(1-\alpha)(1-\delta). \tag{14}$$

In order to conclude the definition of the theoretical impulse response, the instantaneous value of the reverberant field energy at the time $t_D + t_R$, was calculated from Eq. (5), and expressing the time as a function of the distance:

$$g'_R = g'(t_D + t_R) = (31200 \cdot 13.8/V)e^{-(0.04+13.8\rho)r/RT}. \quad (15)$$

The resulting plot of the instantaneous energy density of the theoretical impulse response is shown in Fig. 9.

In order to calculate both strength and clarity, it was necessary to integrate the energy density contributions previously described. The integrated early reflected energy i_E, was calculated as a trapezium area (shaded area in Fig. 9), and was given by:

$$i_E = 0.5t_R(\gamma d + g'_R). \quad (16)$$

The integrated reverberant energy was obtained by putting $t = t_D + t_R$ into Eq. (6):

$$i_L = (31200RT/V)e^{-(0.04+13.8\rho)r/RT}. \quad (17)$$

Since the direct sound energy d is still given by Eq. (7), the total energy can be calculated adding d, i_E, and i_L. However, depending on t_R value, different formulae must be used to calculate the early reflected (e) and late (l) energy with reference to the 80 ms time limit. The simplest method is to calculate e under the assumption that $t_R > 80$, so that the early reflected energy follows the linear law during the whole interval and, after 80 ms, is equal to:

$$g'_{80} = \gamma d - 0.08(\gamma d - g'_R)/(\rho r). \quad (18)$$

Then, the integrated early energy is given by the trapezium area (see Fig. 9):

$$e = 0.08(\gamma d + g'_{80})/2. \quad (19)$$

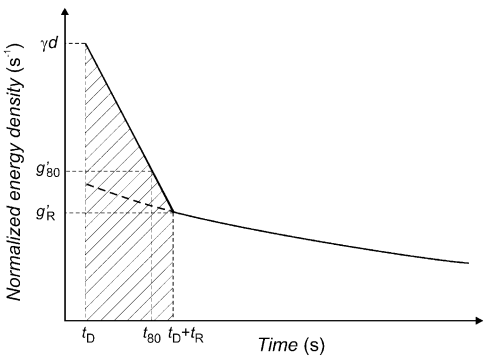

Fig. 9. Plot of the suggested theoretical behaviour of the normalized energy density as a function of time.

Then l is calculated under the assumption that $t_R < 80$ ms, so that the late energy only follows the exponential law throughout the interval and is expressed by means of Eq. (9).

In this way if $t_R > 80$ ms e is given by Eq. (19) and $l = i_E + i_L - e$, otherwise if $t_R < 80$ ms then l is given by Eq. (9) and $e = i_E + i_L - l$. Consequently G and C_{80} may be calculated as usual by means of Eqs. (10) and (11).

As an example of the effects of the new model on different temporal components of sound, Fig. 10 shows the early reflected, late and total energy levels calculated by means of Barron's theory compared with those obtained using the proposed model. It can be seen that the "new" values show a steeper decay as the distance from the source grows. In particular, the "new" early reflected energy is higher than Barron's at points near the source and considerably lower when the distance grows, in agreement with the results shown in Fig. 6. According to Barron's theory both early and late levels vary linearly, whereas the "new" values do not follow linear laws apart from the late level, which varies linearly until $t_R < 80$ ms.

Fig. 11 shows the early level decay trace of points at increasing distances from the source, calculated using the proposed model. A comparison with Fig. 7 shows that there is good agreement with the measured decays.

6. Validation of the model

In order to validate the proposed model, it was applied to the nine churches surveyed. The geometrical data (such as volume, surface area, etc.) were used together with the reverberation time (see Table 1), to determine the coefficients introduced in the previous section (see Table 3). In the two cases of vaulted churches (Barletta and Ognissanti) ρ was increased by a factor 1.25 to account for focusing effects. Then, for every source–receiver combination, the levels of early and late energy and the values of G and C_{80} were calculated using both Barron's model and the proposed one. The results of the calculations were then compared with the data measured in each church by means of three indices: the mean error, the prediction accuracy and the slope difference. The mean error was estimated by the difference between the

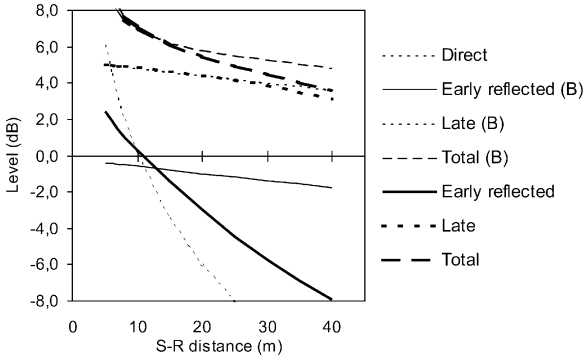

Fig. 10. Theoretical behaviour of the various temporal components of sound energy as a function of source–receiver distance according to Barron's model (B) and to the proposed model (thicker lines). $V = 33\,000$ m^3, RT = 4.4 s, $\gamma = 20$ s^{-1}, $\rho = 5$ ms/m.

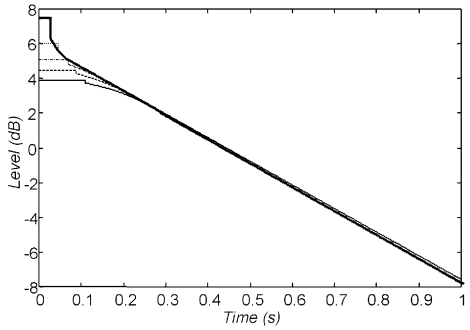

Fig. 11. Theoretical early decay trace calculated at 1 kHz using the proposed model. Different curves correspond to points at different distances from the source. $V = 33\,000\ \mathrm{m}^3$, RT = 4.4 s, $\gamma = 20\ \mathrm{s}^{-1}$, $\rho = 5$ ms/m.

Table 3
Summary of the 1 kHz values of the parameters used to calculate the coefficients ρ and γ

Church	V/S_t (m)	MFP (m)	$\Delta\tau$ (ms)	ϵ (s^{-1})	α	δ	t_{Rmax} (ms)	γ (s^{-1})	ρ (ms/m)
St. Nicholas Basilica, Bari	3.05	12.19	36	28.1	0.11	0.20	255	20.0	6.3
Bari Cathedral	3.17	12.67	37	27.1	0.10	0.20	247	19.6	6.7
Bitonto Cathedral	2.46	9.85	29	34.8	0.09	0.20	180	25.3	5.7
Barletta Cathedral	2.87	11.49	34	29.8	0.07	0.20	179	22.3	6.0[a]
Bisceglie Cathedral	2.18	8.71	25	39.4	0.10	0.25	143	26.6	6.2
Ruvo Cathedral	2.13	8.53	25	40.2	0.09	0.30	114	25.5	5.2
Bovino Cathedral	1.59	6.35	19	54.0	0.08	0.35	88	32.4	5.9
Ognissanti church, Valenzano	1.38	5.54	16	61.9	0.04	0.35	60	38.6	5.1[a]
Vallisa church, Bari	1.35	5.38	16	63.7	0.10	0.40	55	34.3	5.0

[a] ρ values increased by a factor 1.25 to account for focusing vaulted surfaces.

means of measured and predicted values. The prediction accuracy was estimated by the mean rms error between measured and predicted values for each source–receiver combination. Finally, linear regressions for parameter values against the source–receiver distance were performed and the difference between the measured and predicted values of the slopes was determined in dB/10 m. Mean values were calculated excluding the cases where the correlations were not significant at the 5% level.

6.1. Early sound

The proposed model provided significant improvement of prediction accuracy when the early energy level was taken into account. Table 4 shows that the new model reduced the mean error from −2.4 dB, given by Barron's, to −0.5 dB, with a smaller standard deviation which proved its better agreement with the measured data.

This agreement is shown even more clearly by the rms error which, employing the new model, was halved, from 3.3 to 1.5 dB, with a considerable reduction in the standard deviation showing that the improvement is well distributed over the whole sample.

Table 4
Differences between measured and theoretical values of the early energy level based on linear regression with source–receiver distance

Church	Mean (dB)		rms error (dB)		Slope (dB/10 m)	
	Barron	New	Barron	New	Barron	New
St. Nicholas Basilica, Bari	−2.9	−0.3	3.7	0.9	−2.2	−0.1
Bari Cathedral	−3.0	−0.8	3.6	1.6	−1.7	0.6
Bitonto Cathedral	−1.1	0.7	2.1	1.0	−2.3	0.2
Barletta Cathedral	−4.9	−1.0	5.9	2.1	−4.5	−2.1
Bisceglie Cathedral	−1.8	−0.5	3.2	2.1	−4.6	−1.8
Ruvo Cathedral	−2.6	−1.1	3.7	2.0	−4.5	−1.9
Bovino Cathedral	−2.2	0.1	3.0	1.5	−2.6	0.5
Ognissanti church, Valenzano	−2.0	−1.0	2.7	1.5	−4.7	−2.1
Vallisa church, Bari	−1.4	−0.2	1.7	0.8	−1.7	1.2
Mean	−2.4	−0.5	3.3	1.5	−3.2	−0.6
Standard deviation	1.1	0.6	1.2	0.5	1.3	1.3

Mean level differences, rms error and slope differences between measured and theoretical values at 1 kHz frequency band.

Finally, the slope was also predicted with better accuracy when the new model was used. In fact, the mean error was reduced to −0.6 dB/10 m.

A comparison between Figs. 6 and 12 shows that the new early energy level curves fitted the measured data better than Barron's curves.

6.2. Late sound

The effect of the proposed model on the late sound level was less evident than it was for the early sound. This can be seen in Table 5, where the differences between the values provided by the two models are virtually negligible.

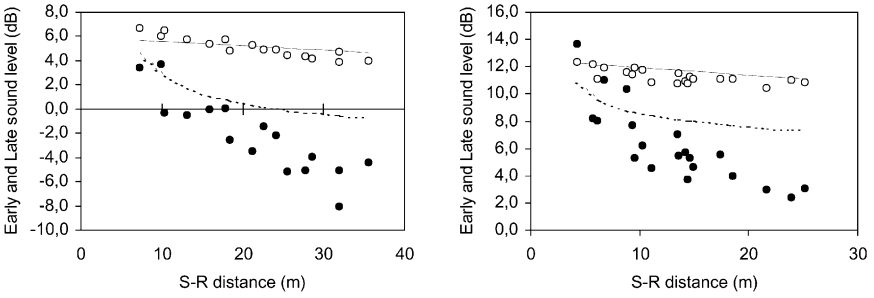

Fig. 12. Plot of predicted (using the proposed model) and measured early and late sound level at 1 kHz octave as a function of the source–receiver distance in Bari Cathedral (left) and Bovino Cathedral (right). (•) measured early level, (- - -) predicted early sound level, (○) measured late sound level, (—) predicted late sound level.

Table 5
Differences between measured and theoretical values of the late energy level based on linear regression with source–receiver distance

Church	Mean (dB)		rms error (dB)		Slope (dB/10 m)	
	Barron	New	Barron	New	Barron	New
St. Nicholas Basilica, Bari	0.6	0.9	0.9	1.0	−0.6	−0.3
Bari Cathedral	−0.1	0.1	0.6	0.5	−0.6	−0.3
Bitonto Cathedral	−0.1	0.0	1.0	0.9	−1.0	−0.8
Barletta Cathedral	0.0	0.2	1.1	1.0	−1.5	−1.3
Bisceglie Cathedral	0.8	0.8	0.9	0.9	−0.2	−0.2
Ruvo Cathedral	−0.7	−0.7	0.8	0.8	−0.6	−0.6
Bovino Cathedral	−0.4	−0.4	0.6	0.6	−0.1	0.0
Ognissanti church, Valenzano	−0.1	−0.1	0.2	0.2	−0.3	−0.3
Vallisa church, Bari	0.0	0.0	0.4	0.4	1.0	1.0
Mean	0.0	0.1	0.7	0.7	−0.7	−0.5
Standard deviation	0.5	0.5	0.3	0.3	0.7	0.6

Mean level differences, rms error and slope differences between measured and theoretical values at 1 kHz frequency band.

This was explained by taking into account that the late sound was affected by the new model only when $t_R > 80$ ms, that is, considering the minimum value of ρ, when the source–receiver distance exceeded about 16 m. In fact, only the four larger churches showed any differences in mean values, while the results were exactly the same in the smaller ones.

It is interesting to observe that the slope differences were often negative, pointing out a steeper decrease with distance of the measured late energy. Fig. 12 shows that this discrepancy could be due to the level measured at points near the source, where it was often higher than that predicted.

6.3. Total sound

Both the analysed models provided similar values of the total sound level at points near the source, while at distant points the new model predicted a steeper decrease (see Fig. 11). As a consequence, the most evident improvement due to the new model was its better prediction of the slope. In fact, Table 6 shows that the mean error and the rms error did not vary significantly when one or the other model was employed, even if, on average, the new model gave better results. However, the slope difference was considerably reduced when the proposed model was used.

Fig. 13 shows the better performance of the proposed model, even if at points near the source the measured level was often higher than the predicted, probably because the theory underestimated the late level at points near the source.

Table 6
Differences between measured and theoretical values of the strength index based on linear regression with source–receiver distance

Church	Mean (dB)		rms error (dB)		Slope (dB/10 m)	
	Barron	New	Barron	New	Barron	New
St. Nicholas Basilica, Bari	0.1	0.8	0.8	0.8	−0.8	−0.2
Bari Cathedral	−0.4	0.2	0.8	0.4	−0.7	−0.1
Bitonto Cathedral	−0.1	0.3	1.1	0.7	−1.2	−0.5
Barletta Cathedral	−0.4	0.2	1.3	1.1	−1.5	−1.1
Bisceglie Cathedral	0.5	0.9	1.3	1.3	−1.9	−1.0
Ruvo Cathedral	−0.9	−0.5	1.3	0.8	−1.6	−1.0
Bovino Cathedral	−0.4	−0.1	0.7	0.5	−1.1	−0.3
Ognissanti church, Valenzano	−0.3	−0.1	0.4	0.3	−0.9	−0.5
Vallisa church, Bari	−0.6	−0.2	0.7	0.5	−0.3	0.6
Mean	−0.29	0.17	0.95	0.7	−1.11	−0.47
Standard deviation	0.39	0.46	0.31	0.34	0.48	0.54

Mean level differences, rms error and slope differences between measured and theoretical values at 1 kHz frequency band.

6.4. Early/late energy ratio

The early to late energy ratio is strongly influenced by the early energy level, therefore the new model considerably improved the prediction accuracy. Table 7 shows this clearly. The mean error was −2.29 dB when Barron's model was used,

Table 7
Difference between measured and theoretical values of the clarity index based on linear regression with source–receiver distance

Church	Mean (dB)		rms error (dB)		Slope (dB/10 m)	
	Barron	New	Barron	New	Barron	New
St. Nicholas Basilica, Bari	−3.5	−1.2	3.9	1.5	−1.5	0.3
Bari Cathedral	−2.8	−0.6	3.2	1.4	−1.3	0.7
Bitonto Cathedral	−1.0	0.9	1.7	1.6	−1.3	1.0
Barletta Cathedral	−5.0	−1.4	5.3	1.6	−2.3	−0.1
Bisceglie Cathedral	−2.0	−0.3	3.1	1.8	−2.9	−0.1
Ruvo Cathedral	−1.7	0.0	2.8	1.4	−3.6	−0.9
Bovino Cathedral	−1.4	−0.2	2.1	1.2	−3.0	0.1
Ognissanti church, Valenzano	−1.6	−0.7	2.2	1.2	−3.7	−1.3
Vallisa church, Bari	−1.6	−0.5	2.0	1.0	−2.5	0.1
Mean	−2.29	−0.45	2.92	1.41	−2.46	−0.01
Standard deviation	1.26	0.66	1.14	0.27	0.94	0.70

Mean level differences, rms error and slope differences between measured and theoretical values at 1 kHz frequency band.

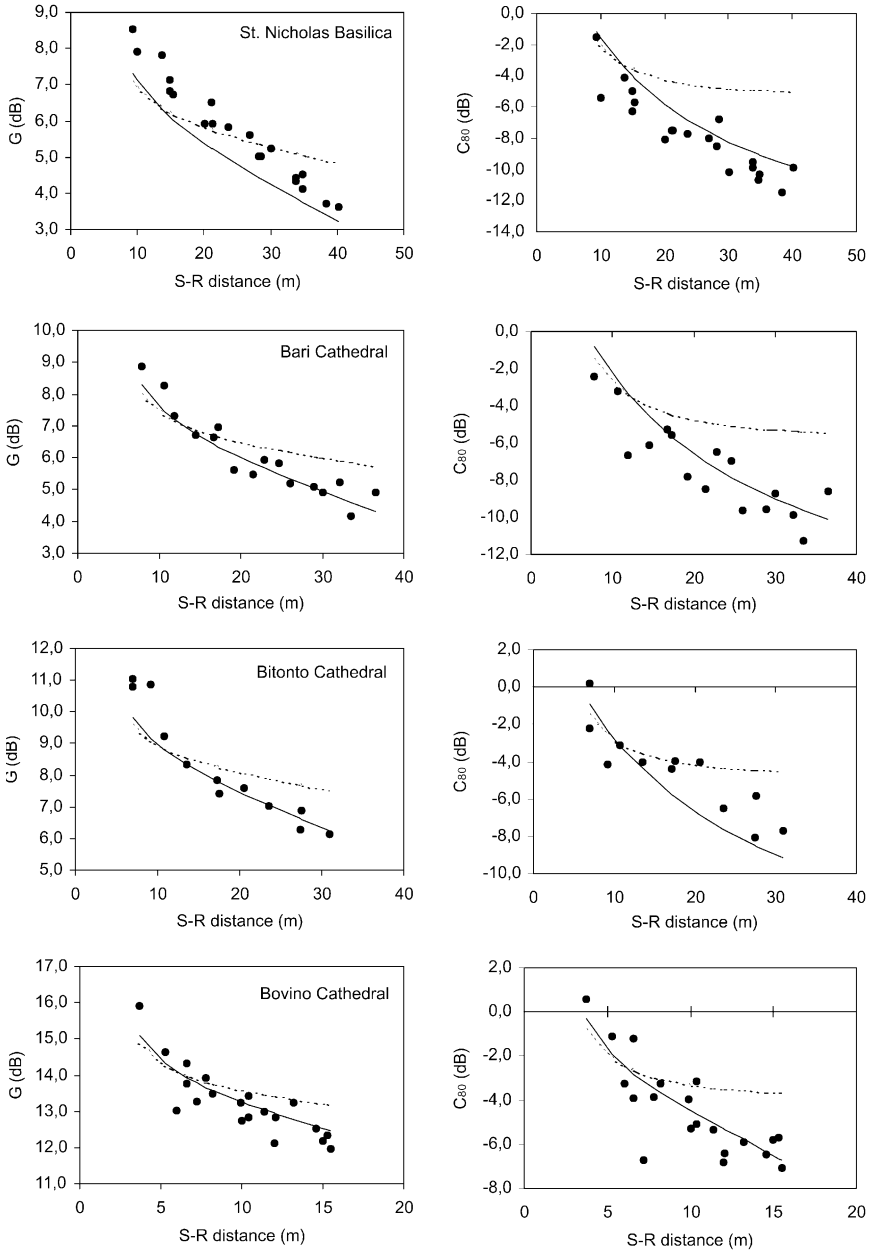

Fig. 13. Plot of measured (•) and predicted values of the strength (left) and clarity (right) index at 1 kHz vs. source-receiver distance in a selected sample of churches. (- - -) Barron's model, and (—) proposed model.

but was reduced to −0.45 dB when the new model was employed. The standard deviation was reduced as well.

The prediction accuracy, given by the rms error, was much better and its mean value was halved and equal to 1.41 dB, with a very small standard deviation.

Finally, the slope difference had much better values when the new model was used and its mean value was −0.01 dB/10 m. Fig. 13 clearly illustrates that the revised model was in considerable agreement with the measured values.

6.5. Frequency dependence

The modifications to the model and all the observations made until now were based on the measurements made at a frequency of 1 kHz. However the performance of the new model at different frequencies was investigated as well. The mean differences between measured and predicted values with reference to both strength and clarity indices were calculated for each frequency band. The results are reported in Tables 8 and 9. First of all it must be said that at 125 and 250 Hz octave bands the measured data were very scattered, and in most of the cases the correlations were not significant. This affected the slope difference which, therefore, lacked significance. However since the measured data do not vary according to a law it makes no sense using any prediction formula. This is proved by the worst performance of the mean difference and, above all, of the rms error regardless of the model adopted for prediction.

Better correlations between measured values and source–receiver distance were found at 500 Hz, even if a significant spread of the data was still present. The rms error was a bit high for the clarity index, however the comparison between the new model and Barron's one showed that the first allows considerably better prediction.

At high frequencies there was significant correlation between measured data and source–receiver distance. This means that the use of a prediction model is reasonable. The new model gave good results in predicting both the total level and early/

Table 8
Summary of the mean, rms and slope differences between measured and theoretical values of the strength index for the six frequency bands

Frequency octave band (Hz)	Mean (dB)		rms error (dB)		Slope (dB/10 m)	
	Barron	New	Barron	New	Barron	New
125	0.41	0.79	1.23	1.36	(−1.13)	(−0.67)
250	0.20	0.59	1.00	1.09	−0.73	−0.19
500	−0.24	0.18	1.12	1.02	−1.17	−0.59
1000	−0.29	0.17	0.95	0.70	−1.11	−0.47
2000	−0.55	−0.03	1.19	0.90	0.39	0.37
4000	−1.03	−0.38	1.57	1.10	−1.31	−0.41
Mean	−0.25	0.22	1.18	1.03	−0.79	−0.26

Slope difference is reported in parentheses if the mean value is based on less than four significant data.

Table 9
Summary of the mean, rms and slope differences between measured and theoretical values of the clarity index for the six frequency bands

Frequency octave band (Hz)	Mean (dB)		rms error (dB)		Slope (dB/10 m)	
	Barron	New	Barron	New	Barron	New
125	−0.52	1.32	2.38	2.92	(−1.51)	(−0.54)
250	−1.69	0.16	2.57	2.14	(−1.96)	(−0.28)
500	−2.81	−0.94	3.56	1.89	−2.64	−0.21
1000	−2.29	−0.45	2.92	1.41	−2.46	−0.01
2000	−2.00	−0.16	2.60	1.51	−2.03	−0.46
4000	−1.60	0.19	2.34	1.55	−1.76	0.72
Mean	−1.82	0.02	2.73	1.90	−2.22	−0.23

Slope difference is reported in brackets if the mean value is based on less than four significant data.

late ratio. At higher frequencies the new model performed better than Barron's in predicting total sound level, giving further evidence of its reliability.

7. Conclusions

After an acoustic survey of nine Apulian-Romanesque churches, the comparison between measured values of strength and clarity and those predicted using Barron's theory, showed considerable differences. It was observed that the early sound level decrease with distance was steeper than predicted. This was explained by assuming that most of the room surfaces were highly scattering, therefore early reflections were stronger near the source and weaker at farther positions. This observation led to modifying Barron's model introducing two assumptions: the linear reverberant level decay does not start at the moment of arrival of the direct sound, but after a time proportional to the source–receiver distance; the early reflection energy density follows a simple linear law from an initial energy value (proportional to the direct sound), to the value of the reverberant field energy at the time it starts.

The factors influencing the reverberation start-up time and the initial early energy value were found to depend on simple geometrical and acoustic characteristics mostly derived from the classical theory, and can be easily calculated for each room. This allows the proposed model to be considered not merely empirical but based on theoretical assumptions.

The performance of the new model was tested by comparing the values of early, late and total sound level, and the early/late energy ratio with those measured. Barron's values were calculated as well and used as a reference. Good results were achieved, and the rms errors for strength and early/late ratio were respectively equal to 0.7 and 1.4 dB, the latter being nearly the half of the error given by Barron's theory.

The new model was tested over six octave bands but it proved to be reliable only at mid and high frequencies. At low frequency the measured data appeared too scattered to be correlated with source–receiver distance, therefore a prediction model was of little practical use in that case. In order to have a definite validation of the model, further investigations are required and a new survey is under way. Churches of different architectural style, of different typology and, possibly, completely different kind of rooms, such as concert halls, will be analysed. The application of the model to predict other acoustic parameters, such as centre time and early decay time, will be the subject of later articles.

Acknowledgements

The authors wish to thank all the parish priests and church management for allowing access to their churches.

References

[1] Raes AC, Sacerdote G. Measurement of the acoustical properties of two roman basilicas. J Acoust Soc Am 1953;25(5):925–61.
[2] Shankland RS, Shankland HK. Acoustics of St. Peter's and patriarchal basilicas in Rome. J Acoust Soc Am 1971;50(2):389–95.
[3] Fearn RW. Reverberation in Spanish, English, and French churches. J Sound Vib 1975;43(3):562–7.
[4] Mijic M. Serbian Orthodox Church—an acoustical view. In: Proc. 17th ICA, Rome; 2001.
[5] Lewers TH, Anderson JS. Some acoustical properties of St. Paul Cathedral, London. J Sound Vib 1984;92(2):285–97.
[6] Desarnaulds V, Bossoney S, Eggenschwiler K. Studie zur Raumakustik von Schweizer Kirchen. In: Fortschritte der Akustik—DAGA 98, Zürich; 1998. p. 710–11.
[7] Carvalho APO. Relations between rapid speech transmission index (RASTI) and other acoustical and architectural measures in churches. Applied Acoustics 1999;58:33–49.
[8] Sendra JJ, Zamarreño T, Navarro J. Acoustics in churches. In: Sendra JJ, editor. Computational acoustics in architecture. Southampton: Computational Mechanics Publications; 1999. p. 133–77.
[9] Galindo M, Zamarreño T, Giron S. Clarity and Definition in Mudejar-Gothic Churches. Building Acoustics 1999;6:1–16.
[10] Prodi N, Marsilio M, Pompoli R. On the prediction of reverberation time and strength in mosques. In: Proc. 17th ICA, Rome; 2001.
[11] Sendra JJ, Zamarreño T, Navarro J, Giron S, Galindo M. Acoustical Behaviour in Mudejar-Gothic Churches. In: Proc. 17th ICA, Rome; 2001.
[12] Anderson JS, Bratos-Anderson M. Acoustic coupling effects in St Paul's Cathedral, London. J Sound Vib 2000;236(2):209–25.
[13] Cirillo E, Martellotta F. Acoustics of Apulian-Romanesque churches: correlations between architectural and acoustic parameters. Building Acoustics [submitted for publication].
[14] Barron M, Lee LJ. Energy relations in concert auditoriums. I. J Acoust Soc Am 1988;84(2):618–28.
[15] Martellotta F. Caratteristiche acustiche delle chiese romaniche in Puglia. Doctoral thesis in Applied Physics, Università degli Studi di Ancona; 2001 [in Italian].
[16] Cremer L, Muller HA. Principles and applications of room acoustics, vol. 1. London: Applied Science; 1982.
[17] Arau H. General theory of the energy relations in halls with asymmetrical absorption. Building Acoustics 1998;5(3):163–83.

[18] Gade AC. The influence of architectural design on the acoustic of concert halls. Applied Acoustics 1990;31:207–14.
[19] ISO-3382. Acoustics—measurement of the reverberation time of rooms with reference to other acoustical parameters; 1997.
[20] Kuttruff H. Room acoustics. 3rd ed. London: E & FN Spon; 1991.